Thermal Management of Vehicle Electronic Payloads Using Nanofluids and Thermoelectric Devices — Modeling and Analysis

Authors:

David J. Ewing, Joshua Finn, Lin Ma, PhD., John Wagner, PhD., PE.

Affiliation:

Clemson University, Department of Mechanical Engineering, Clemson, SC 29634

Abstract

Electronic payloads have become an integral part of modern military ground vehicles. These electronics often feature high thermal density that must be effectively managed, especially under demanding operating conditions, to maintain system reliability. This paper describes the modeling and analysis of nanofluids and thermoelectric devices to address the cooling challenges posed by these thermal loads. A sensitivity analysis has been performed to investigate the suitability of a particular nanofluid model. Numerical results obtained show that the convective heat transfer coefficient can be enhanced up to 16.1% with the augmentation of nanoparticles into the base fluid (water). The simulation results also show that the peak computer chip temperature varies by only 0.4%, demonstrating that it is insensitive to the complexity of the selected nanofluid model. Furthermore, the proposed thermal management system provides cooling performance which would not be possible with traditional air-cooled heat sinks which remain limited to the ambient temperatures.

Keywords: Nanofluid; thermoelectric; thermal modeling sensitivity; military electronic cooling; coolant rail; nanoparticles; peak temperature suppression; nodal modeling; effective properties

1 Introduction

Report Documentation Page

Form Approved
OMB No. 0704-0188

1. REPORT DATE	2. REPORT TYPE	3. DATES COVERED
01 MAR 2011	**N/A**	**-**

4. TITLE AND SUBTITLE	5a. CONTRACT NUMBER
Thermal Management of Vehicle Electronic Payloads Using Nanofluids and Thermoelectric Devices--Modeling and Analysis (PREPRINT)	**W56HZV-04-2-0001**
	5b. GRANT NUMBER
	5c. PROGRAM ELEMENT NUMBER
6. AUTHOR(S)	5d. PROJECT NUMBER
David J. Ewing; Jouhua Finn; Lin Ma PhD; John Wagner,PhD.,PE	5e. TASK NUMBER
	5f. WORK UNIT NUMBER
7. PERFORMING ORGANIZATION NAME(S) AND ADDRESS(ES)	8. PERFORMING ORGANIZATION REPORT NUMBER
Clemson University, Department of Mechanical Engineering, Clemson, SC 29634	
9. SPONSORING/MONITORING AGENCY NAME(S) AND ADDRESS(ES)	10. SPONSOR/MONITOR'S ACRONYM(S)
US Army RDECOM-TARDEC 6501 E 11 Mile Rd Warren, MI 48397-5000, USA	**TACOM/TARDEC/RDECOM**
	11. SPONSOR/MONITOR'S REPORT NUMBER(S) **21547**

12. DISTRIBUTION/AVAILABILITY STATEMENT
Approved for public release, distribution unlimited

13. SUPPLEMENTARY NOTES
Submitted for publication in a Special Issue of Int'l Journal of Vehical Design

14. ABSTRACT

15. SUBJECT TERMS

16. SECURITY CLASSIFICATION OF:			17. LIMITATION OF ABSTRACT	18. NUMBER OF PAGES	19a. NAME OF RESPONSIBLE PERSON
a. REPORT **unclassified**	b. ABSTRACT **unclassified**	c. THIS PAGE **unclassified**	**SAR**	**28**	

Modern military ground vehicles, such as Force Protection's Cougar MPAV, may carry a vast array of electronic equipment to perform command and control tasks that require reliable temperature control to maintain system integrity. Computer hardware continues to evolve with greater computational abilities and progressively smaller package sizes for a given power density which raises the heat load on the overall system. Particularly in defense applications, electronic systems may be operated in a wide range of conditions, including hot desert climates where heat rejection is difficult due to the decreased differential between the ambient conditions and the equipment's maximum operating temperature. To ensure adequate cooling in adverse environments, a thermal management system must be developed which is capable of adequately cooling the electronics while maintaining packaging flexibility and reliable operation in combat environments.

Thermal management technology for automotive applications has begun to use computer controlled electro-mechanical components for enhanced temperature control (Mitchell, et al., 2009). Liquid cooling systems lend themselves well to heat transfer in electronic equipment and are, in fact, currently being used in several computer server and after-market computational systems (Ellsworth, et al., 2008). Electrically powered cooling components may be controlled to maintain prescribed temperatures and reduce power consumption (Pfahnl and Liang, 2004). Recent developments, and accompanying mathematical models, in heat exchanger design allow improved convective heat transfer coefficients with better insights into their operation (Robinson, 2009, Tan, et al., 2007). The primary limitation, however, of standalone liquid cooling remains the required temperature differential over the ambient conditions which may result in unacceptable device operating temperatures in hot climates.

Peltier effect thermoelectric coolers (TEC) have demonstrated attractive cooling properties for computational applications since they can cool these system components below ambient temperatures in certain operating regimes (Simons and Chu, 2000). The heat transfer process occurs without moving parts in the TEC module, thus providing a distinct advantage over conventional vapor compression cycles. The cooling effect in Peltier devices is achieved by a current flow through the junction of two dissimilar materials. The cooling available from TEC's has enabled processor overclocking capabilities in certain applications (Wang, Zou and Friend, 2009). Additionally, larger TEC's may serve multiple computer chips, such as in multi-core processing, as demonstrated by (Simons, Ellsworth and Chu, 2005). However, an effective means must exist to reject heat to the TEC module and overcome the generated heat flux.

The successful operation of the TEC system is dependent on the heat rejection accommodations of the supplemental cooling system. A high capacity cold reservoir is required for optimal heat rejection. This goal may not be a significant design issue when space requirements are not imposed, and passive cooling systems such as free convection may be implemented (Lertsatitthanakorn, et al., 2001). More conventional installations, such as the ones demonstrated by (Chang, et al., 2009), use forced convection and have proven to yield adequate performance. Space limitations, however, often demand the implementation of different cooling technologies, and new electronic systems may feature higher power densities such that direct air cooling cannot meet the heat rejection demands. Liquid cooling has proven capable of meeting these demands and is well suited for thermoelectric systems (Huang, et al., 2010).

The performance of liquid cooling systems can often be improved through the addition of suspended particulates. Experiments have shown that, by adding nanoparticles

with much higher thermal conductivity than the base fluid, the thermal transfer properties of the base fluid are enhanced (Choi, 2009, Godson, et al., 2010, Kakac and Pramuanjaroenkij, 2009, Nguyen, et al., 2007, Wang and Mujumdar, 2007, Wong and Kurma, 2008, Wong and Castillo, 2010). This heat transfer improvement is attractive for use in thermal management systems, such as car radiators (Leong, et al., 2010), by providing increased thermal protection for mission critical components. However, the actual nanofluid mechanisms are still debated due to the inconsistencies present in the available experimental data and the widely varying models that have been developed (Godson, et al., 2010, Kakac and Pramuanjaroenkij, 2009, Wang and Mujumdar, 2007, Wong and Castillo, 2010). The accurate mathematical modeling of nanofluids remains a debated and uncertain area of research. Due to this uncertainty, it is highly desirable to directly compare the influence of multiple nanofluid models in simulations in order to study their significance.

The development of an integrated liquid and TEC cooling system with nanofluid particles should offer greater design flexibility and modular designs for small electronics packages. This approach should be well suited to military and avionics applications where space limitations and high ambient temperatures make cooling difficult. The implementation of multiple cooling loops so that the thermoelectrics are not in direct contact with their respective electronic heat loads can eliminate condensation problems and minimize the cooling footprint on the actual electronic component. Nanofluids should enhance the cooling performance and reduce the thermal resistance throughout the multiple loop system. Also, investigation of nanofluid modeling techniques will provide insight into the effectiveness of various models and demonstrate the effectiveness of the proposed cooling system. The remainder of the paper has been organized as follows. Section 2 presents the fundamental concepts of nanofluid modeling. Thermoelectric modeling concepts are provided in Section 3. A thermal system model is introduced in Section 4 for an electronic system case study

featuring computer chips and cooling components operating in extreme conditions. The nanofluid models and thermoelectric devices are applied for temperature regulation of a computer chip with full discussion of the representative numerical results. Finally, the summary is contained in Section 5.

2 Fundamentals and Modeling of Nanofluids

The issue of cooling electronic payloads has been approached by modeling a system containing combined thermoelectric and nanofluid technologies to achieve maximum thermal protection and packaging flexibility. The critical issue of nanofluids property modeling will be discussed with the introduction of three approaches – classical, Brownian motion, and empirical data curve fit.

2.1 Nanofluids

Nanofluids have been a source of research for the past several years due to their observed ability to enhance the thermal transfer properties of base fluid properties (Chandrasekar and Suresh, 2009, Choi, 2009, Godson, et al., 2010, Kakac and Pramuanjaroenkij, 2009, Wong and Kurma, 2008). Micron-sized particles were originally used in research for enhancing the heat transfer properties of cooling fluids; however, these particles were deemed impractical for many applications since the resultant fluid required large increases in pumping power and also increased the pipe wall friction which lead to greater pipe wear (Choi, 2009). However, as research progressed, nano-sized particles were introduced into these systems and they enhanced the thermal transfer characteristics while greatly reducing the negative aspects of pumping power and pipe wear, making nanofluids a much more viable option to use in practical thermal protection systems (Choi, 2009).

While these benefits have been well documented, the actual nanofluid mechanisms are still debated (Chandrasekar and Suresh, 2009, Choi, 2009, Godson, et al., 2010, Kakac

and Pramuanjaroenkij, 2009, Wong and Kurma, 2008, Wong and Castillo, 2010). As revealed from these references, inconsistencies in the experimental data as well as the wide range of models available regarding nanoparticle enhancement of base fluids remain the primary causes of this ongoing debate. While thermal fluids property improvements have been shown to depend on the shape, size, and concentration of the nanoparticles, the underlying mechanisms have yet to be conclusively decided. Among existing models, the more prominent descriptions include classic models such as Maxwell's equation for thermal conductivity and Einstein's model for viscosity (Chandrasekar and Suresh, 2009, Nguyen, et al., 2008), Brownian motion (Batchelor, 1977, Prasher, Bhattacharya and Phelan, 2005), or simply the utilization of data curve fitting (Wong and Kurma, 2008). The importance of the latter two models is shown by the strong temperature dependence demonstrated by the nanofluids (Nguyen, et al., 2008, Wong and Kurma, 2008). These facts, along with the data inconsistencies, create difficulties in modeling the nanoparticle effects on the thermal transfer properties of their base fluids. Consequently, the modeling of nanofluids remains an unresolved research area.

Another difficulty in modeling the overall convective heat transfer coefficient, *h*, for the nanofluids is that few studies have been performed to evaluate the viscosity increases of the base fluids by the addition of nanoparticles (Duangthongsuk and Wongwises, 2009, Godson, et al., 2010, Kakac and Pramuanjaroenkij, 2009, Nguyen, et al., 2008, Wong and Kurma, 2008). Although analyses on the combined effects of the nanofluid's thermal conductivity and viscosity have been performed in select systems, they must ideally be established for each proposed application. A practical need exists to establish the sensitivity of nanofluid models used in the thermal management system within the paper. The models investigated to describe the nanofluid thermal transfer process include a simple classic, Brownian motion effects, and experimental curve fitting.

2.2 Nanofluid Models

As mentioned previously, the modeling of nanofluids remains challenging due to the lack of consistent data and the continued debate concerning the underlying mechanisms of nanofluid thermal transfer. Therefore, a sensitivity analysis of the proposed nanofluid models will be performed to observe the individual model's effect on the maximum temperature and the transient temperature profile of the given thermal load (e.g. computer chips). This analysis should offer insight into the importance of nanofluid model selection while examining both the thermal conductivity and the viscosity. Models which offered uniform treatment of the thermal transfer enhancement were chosen to describe the effective thermal conductivity and the effective viscosity of the nanofluid (i.e. from the classes of classic volume fraction models, Brownian motion models, and experimental curve fitting).

The first analysis task was to determine the size of the nanoparticles for the proposed system. Figure 1 shows the size distribution of the suggested nanoparticles; the mean diameter of the nanoparticles was 46 nm. It is important that the size distribution of the proposed nanoparticles remained consistent with the sizes used in several previous studies, including (Wong and Kurma, 2008), to ensure consistent modeling conditions. The Dittus-Boelter equation was used to model the Nusselt number relationship shown in Equation (1) (Incropera and DeWitt, 1990) to provide a consistent model for the convective heat transfer coefficient

$$Nu = 0.023 \mathrm{Re}_D^{0.8} \mathrm{Pr}^{0.4} \quad (1)$$

In this expression, the term Nu is the Nusselt number, Re_D is the Reynolds number ($Re_D=\rho VD/\mu$), Pr is the Prandtl number ($Pr=c_p\mu/k$), ρ is the density of the base fluid, D is the diameter of the pipe being used, μ is the dynamic viscosity, c_p is the specific heat capacity,

and k is the thermal conductivity. From Nu, the convective heat transfer coefficient, h, may be calculated using Equation (2).

$$h = \frac{kNu}{D} \tag{2}$$

2.2.1 Classic Model

The first sensitivity analysis model is based on some classical model features for the effective thermal conductivity and viscosity of the nanofluid. This approach considers the volume fraction of the nanoparticles. The mathematical description for the effective thermal conductivity of the nanofluid has been listed in Equation (3) (Wang and Mujumdar, 2007)

$$k_{eff} = \frac{k_p + 2k_f + 2\phi\ (k_p - k_f)}{k_p + 2k_f - \phi\ (k_p - k_f)} k_f \tag{3}$$

In this equation, k_p is the nanoparticle thermal conductivity, k_f is the base fluid thermal conductivity, k_{eff} is the effective thermal conductivity of the nanofluid, and ϕ is the volume fraction of the nanoparticles. In the latter instance, ϕ = 8.47% was assumed for consistency with the study preformed in (Wong and Kurma, 2008) as discussed in Section 2.2.3.

To describe the effective viscosity of the nanofluid, the model was formulated based on Einstein's work and shown in Equation (4) (Nguyen, et al., 2008).

$$\mu_{eff} = (1 + 2.5\phi)\ \mu_f \tag{4}$$

In this equation, μ_{eff} is the effective viscosity, and μ_f is the base fluid viscosity.

2.2.2 Brownian Motion Model

The second model chosen to represent the nanofluid behavior was based upon the interaction of the particles and the fluid caused by Brownian motion. According to (Prasher, Bhattacharya and Phelan, 2005), the mechanism that Brownian motion causes is micro-convection within the base fluid. The proposed model for the effective thermal conductivity has been shown in Equations (5) and (6) (Prasher, Bhattacharya and Phelan, 2005)

$$k_{eff} = k_f \left(1 + A\,\mathrm{Re}^m\,\mathrm{Pr}^{0.333}\,\phi\right)\left[\frac{1+2\alpha+2\phi(1-\alpha)}{1+2\alpha-\phi(1-\alpha)}\right] \tag{5}$$

where

$$\alpha = \frac{2R_b k_m}{d_N} \quad and \quad \mathrm{Re} = \frac{1}{\nu}\sqrt{\frac{18k_b T}{\pi\rho_N d_N}} \tag{6}$$

In these two equations, *Re* is the Reynolds number based upon the base fluid flowing around the nanoparticle, *Pr* is the Prandtl number of the base fluid, R_b is the interfacial thermal resistance between the nanoparticle and the fluid, k_b is the Boltzmann constant, T is the temperature of the fluid, ν is the kinematic viscosity of the base fluid, ρ_N is the density of the nanoparticle, d_N is the diameter of the nanoparticle, k_m is the matrix thermal conductivity, A is a fitting parameter independent of base the fluid, and m is a fitting parameter dependent of the base fluid. The values of R_b, A, and m were adapted from the values given in (Prasher, Bhattacharya and Phelan, 2005).

For the effective viscosity of the nanofluid considering Brownian motion, the model developed by (Batchelor, 1977), given in Equation (7), was utilized

$$\mu_{eff} = \left(1 + 2.5\phi + 6.5\phi^2\right)\mu_f \tag{7}$$

2.2.3 Experimental Data Model

The final senstivity analysis model considered was based on curve fitting experimental data presented in (Wong and Kurma, 2008). The authors presented experimental data for several volume fractions of nanoparticles for both thermal conductivity and viscosity at various nanofluid temperatures. The data indicated a linear increase in thermal conductivity with an increase of temperature, while the viscosity decreased exponentially. The volume fraction of ϕ = 8.47% was used to find the effective thermal conductivity and viscosity. The curve equations for the thermal conductivity and viscosity have been summarized in Equations (8) and (9)

$$k_{eff} = 0.0024T + 0.6275 \tag{8}$$

$$\mu_{eff} = 3\times10^{-6} e^{-0.023T} \tag{9}$$

3 Thermoelectric Model

The heat transfer behavior of a Peltier effect device, illustrated in Figure 2, is generally regulated by the flow of current, *i*, through the unit. The current flow is dependent on both the unit's electrical properties and the hot and cold side temperatures. Thus, the relationship for current depends on the unit supply voltage, V_i, electrical resistance, R_{TEC}, and the temperatures of the two plates, T_H and T_C, as shown in Equation (10).

$$i = \frac{1}{R_{TEC}} V_i \; - \alpha \; T_H + T_C \; \cong \frac{1}{R_{TEC}} V_i \tag{10}$$

The parameter α denotes the Seibec coefficient of the thermoelectric material (note that $\alpha < 0$) (Dai, Wang and Ni, 2003). Since α is small, its effect may be neglected for ease of analysis in this case. The power, *P*, consumed by the thermoelectric device may be expressed in Equation (11).

$$P = i^2 R_{TEC} + \alpha i R_{TEC} \ \ T_H + T_C \ \ \cong i^2 R_{TEC} \tag{11}$$

The heat removal equation for the cold side of the TEC can be described based on the electrical resistance, Peltier effect, and thermal conductivity so that the heat removed, $\dot{Q}_{cold}$, is given in Equation (12) by (Baumann, 2006)

$$\dot{Q}_{cold} = -2n \ \ \alpha i T_{avg} \ \ - \frac{1}{2} i^2 R_{TEC} - A_{TEC} k_{TEC} \ \ T_H - T_C \tag{12}$$

In this expression, $T_{avg} = 0.5 \ \ T_H + T_C \ \ $, and n is the number of thermoelectric couples in the TEC. The parameter α may not be neglected from Equation (12) since n is sufficiently large ($n \approx 10^2$). Using Ohm's law, the heat transfer behavior may be expressed in Equation (13) in terms of the supply voltage.

$$\dot{Q}_{cold} = -2n \ \ \alpha T_{avg} \ \ \frac{V_i}{R_{TEC}} - \frac{1}{2} \frac{V_i^2}{R_{TEC}} - A_{TEC} k_{TEC} \ \ T_H - T_C \tag{13}$$

For TEC devices, the thermal conductivity influences both the hot and cold side temperatures, and the resistance heat is shared. The heat added to the component's hot side may be written in Equation (14) as (Riffat and Ma, 2003)

$$\dot{Q}_{hot} = -2n \ \ \alpha T_{avg} \ \ \frac{V_i}{R_{TEC}} + \frac{1}{2} \frac{V_i^2}{R_{TEC}} + A_{TEC} k_{TEC} \ \ T_H - T_C \tag{14}$$

A power-saving strategy has been implemented in the thermoelectric system so that the devices operate when their respective CPU's experience an elevated temperature. The control structure in Equation (14) takes the form of a digital thermostat so that the unit's supply voltage, V_i, becomes

$$V_i = \begin{Bmatrix} V & ; & T_C \geq T_{in,i} + T_{high} \\ V\left(\dfrac{T_C - T_{in,i} - T_{low}}{T_{high} - T_{low}}\right) & ; & T_{in,i} + T_{low} < T_C < T_{in,i} + T_{high} \\ 0 & ; & T_C \leq T_{in,i} + T_{low} \end{Bmatrix} \quad (15)$$

4 Case Study – Nanofluid Based Thermoelectric Cooling System

The nanofluid models previously discussed in Section 2 will be combined with thermoelectric devices from Section 3 and applied to a mobile electronic system subject to desert operating conditions to evaluate cooling effectiveness. The overall performance will be assessed by studying the temperature profile and peak temperatures of the computer chips as well as the increase of the convective heat transfer coefficient. Also, the sensitivity of the system response will be evaluated by comparing the peak temperatures of the three nanofluid models utilized. To begin the case study, the vehicle electronics system will be described with an accompanying mathematical model. This system was designed with multiple coolant loops to enable modular design and maximize packaging flexibility for space limited applications, as shown in Figure 3. This flexibility is achieved by isolating the thermoelectric devices from their respective computer chips so that pressure mounting hardware need not be applied to the circuit board.

4.1 Vehicle Electronic Thermal Management Model

Nodal equations may be used to describe the thermal response of each of the system's primary components as illustrated in Figure 3. A lumped capacitance model uses a set of ordinary differential equations representing the various temperature nodes. This method models the heat transfer process based upon the thermal resistances, R_i, and the heat capacitances, C_j within the system. Thus, the thermal response of the *jth* thermal node, T_j, may be stated in Equation (16) as

$$C_j \dot{T}_j = \sum_i \frac{1}{R_i} \left(T_i - T_j \right) + \dot{Q}_j, \quad j = 1, 2, ..., n \tag{16}$$

where $\dot{Q}_j$ is the corresponding heat load, and n is the total number of nodes. For this model, thermal resistances, R_i, consider both convection and conduction heat transfer while neglecting radiation effects. The nanofluid properties are temperature dependent and must be carefully treated within the computer algorithm. An example formulation considers the interaction between an inner coolant loop and two TEC nodes which may be described by Equation (17)

$$\begin{aligned} C_{cool,in,i} \dot{T}_{cool,in,i} &= \frac{1}{R_{cool,in,i}} \left(T_{cold,i} - T_{cool,in,i} \right) + \frac{1}{R_{cool,in,i}} \left(T_{C,i} - T_{cool,in,i,i} \right) \\ C_{cold,i} \dot{T}_{cold,i} &= \frac{1}{R_{cool,in,i}} \left(T_{cool,in,i} - T_{cold,i} \right) - \dot{Q}_{cold,i} \\ C_{hot,i} \dot{T}_{hot,i} &= \frac{1}{R_{cool,out}} \left(T_{cool,out} - T_{hot,i} \right) + \dot{Q}_{hot,i} \end{aligned} \tag{17}$$

In this expression, the subscript *C,i* denotes the *ith* CPU node, $T_{cool,in,i}$ is the average temperature of the associated inner coolant loop, and $T_{cool,out}$ is the average temperature of the outer cooling loop. The convective thermal resistances are defined as $R_{cool,in,i} = 1/(A_{cool,in} h_{cool,in,i})$ and $R_{cool,out} = 1/(A_{cool,out} h_{cool,out})$, where A is the surface area of the associated heat exchanger, and h is the convective heat transfer coefficient. The interfacial thermal contact resistance of the TEC/heat exchanger interface is negligible when compared to the other system thermal resistances and so has been ignored.

The standard formulations for the convective and conductive thermal resistances have been implemented and the nodes compiled into a suite of nodal equations (Finn, et al., 2010). The state-space formulation has the form $\dot{\vec{x}} = A\vec{x} + B\vec{u}$ with the state and input vectors, $\vec{x} \in \Re^{17 \times 1}$ and $\vec{u} \in \Re^{7 \times 1}$, respectively.

4.2 Test Conditions

The effect of the three nanofluid models described in Sections 2.2.1-2.2.3 on the system response was studied in the proposed multiple loop cooling system. The high temperature ambient conditions were provided based on a cyclic pattern for desert climates. A variable heat load was imposed by setting the individual computers to cycle on and off during the 24 hour time interval considered. This procedure resulted in the step changes shown in Figure 4 with the maximum load being allowed to coincide with the peak ambient temperature. The changes in heat load allow for observation of the transient behavior of the system as would be observed in actual operation. The system parameter values were determined from material properties, geometry, and environmental conditions. The model was simulated in the Matlab/Simulink environment with an integration time step of Δt = 0.10 s. A complete summary of the modeling parameters are given in Table 1. For ease of reference, a flow chart is presented in Figure 5 to show the order of the simulation process.

4.3 Thermal Protection – Transient Computer Temperature Analysis

The thermal management system limited the peak temperature of the computer chips. In Figure 6, the transient temperature profile has been displayed for a single computer chip for the given 24 hour operating period using water (Base Fluid), the Classical Model (Classic Form), the Brownian Motion Model (Brownian Motion), and the Experimental Data Model (Fit from Wong and Kurma). Table 2 summarizes the maximum computer chip temperatures, nanofluid temperatures, and convective heat transfer coefficient values. From Figure 6 and Table 2, it can be observed that the nanofluids only decreased the peak computer chip temperature by 0.6^0C. The reason for this small temperature difference will be discussed in Section 4.4. However, it can also be clearly observed that there is no significant difference in the peak computer chip temperature between the three nanofluid models. This observation is important since it demonstrates that with this system, considering the overall

goal of peak temperature limitation of computer chips, the selected nanofluid model has little effect.

4.4 Thermal Protection – Enhancement of the Convective Heat Transfer Coefficient

The convective heat transfer coefficient has been significantly enhanced by the utilization of nanofluids. Figure 7 shows the temperature dependent profile of the convective heat transfer coefficient for each nanofluid model. All models offered a large improvement over the base fluid (water) model, especially as the temperature increased. Figure 8 displays the maximum percentage increase of the convective heat transfer coefficient, h, in comparison to the base fluid (water) for each model. From these two figures and Table 2, the heat transfer coefficient can be enhanced by up to 16.1%, demonstrating that augmenting ordinary cooling fluids with nanoparticles can be extremely advantageous in many thermal protection applications.

As noted earlier, however, the limitation of peak computer chip temperature seems to remain relatively unchanged, even with increased convective heat transfer coefficients. This occurrence can be explained by two possible factors. First, the contact area between the coolant rail and the computer is quite small due to the enclosure restraints for this application. Therefore, an enhancement in the convective heat transfer coefficient would be less noticeable given the small contact area. Second, for the given system heat input and fixed contact area, the temperature difference between the fluid and the computer is already quite small (refer to Table 2). Therefore, a 16.1% increase in the convective heat transfer coefficient will only translate into a 16.1% decrease in the temperature difference. In this system, this translates into a small change in the peak computer chip temperature. Therefore, for this application where the solution is insensitive to the model chosen, the Classic Model would be preferred for its simplicity. However, if the system heat input increases, then the

advantages of using nanofluids in the coolant system would become more evident. Also, the contact area between the nanofluid and the computer chip assembly may be decreased in order to further decrease the footprint of the cooling system in confined spaces. Therefore, while the peak computer chip temperature is only slight decreased by the use of nanofluids, the increase observed in the convective heat transfer coefficient demonstrates the unique advantages of nanofluids.

5 Summary

The demanding cooling issues in vehicular electronic payloads such as those used in military ground vehicles have been addressed by augmenting a thermoelectric cooling system with nanofluids in a configuration which maximizes packaging flexibility and cooling effectiveness. Since nanofluid modeling remains an unresolved research topic, three nanofluid models were chosen and compared to a base cooling fluid (water) to determine the significance of the particular nanofluid model utilized and the overall effectiveness of the nanofluids compared with the base fluid. When simulated for desert operating conditions, the system showed favorable cooling performance; however, there was little change in the peak computer chip temperature when using nanofluids as opposed to the base fluid. Despite the significantly increased convective heat transfer coefficient (up to 16.1%) for nanofluids, the effect is minimized by small contact area in the heat sinks and small heat input. Additionally, the various nanofluid models showed little difference (< 0.4%) in peak temperature, demonstrating insensitivity to the chosen nanofluid model. Due to the increase in the heating demands of modern electronic devices, these findings should be of particular interest in the augmentation of current heat transfer strategies.

References

Batchelor, G.K. (1977) 'Effect of Brownian-motion on bulk stress in a suspension of spherical-particles', *Journal of Fluid Mechanics*, Vol. 83, pp. 97-117.

Baumann, J. (2006) 'Modeling and sizing a thermoelectric cooler within a thermal analyzer'. *Paper presented at the Annual Spacecraft Thermal Control Workshop. Mar. 2006*. El Segundo, CA.

Chandrasekar, M. and Suresh, S. (2009) 'A review on the mechanisms of heat transport in nanofluids', *Heat Transfer Engineering*, Vol. 30, No. 14, pp. 1136-1150.

Chang, Y.W., Chang, C.C., Ke, M.T. and Chen, S.L. (2009) 'Thermoelectric air-cooling module for electronic devices', *Applied Thermal Engineering*, Vol. 29, No. 13, pp. 2731-2737.

Choi, S.U.S. (2009) 'Nanofluids: From Vision to Reality Through Research', *Journal of Heat Transfer-Transactions of the ASME*, Vol. 131, No. 3, pp. 033106-1-033106-9.

Dai, Y.J., Wang, R.Z. and Ni, L. (2003) 'Experimental investigation and analysis on a thermoelectric refrigerator driven by solar cells', *Solar Energy Materials and Solar Cells*, Vol. 77, No. 4, pp. 377-391.

Duangthongsuk, W. and Wongwises, S. (2009) 'Measurement of temperature-dependent thermal conductivity and viscosity of TiO2-water nanofluids', *Experimental Thermal and Fluid Science*, Vol. 33, No. 4, pp. 706-714.

Ellsworth, M.J., Campbell, L.A., Simons, R.E. and Iyengar, R.S.S. (2008) 'The evolution of water cooling for IBM large server systems: Back to the future'. *Paper presented at the Intersociety Conference on Thermal and Thermomechanical Phenomena in Electronic Systems, ITHERM. May 28-31, 2008*. Orlando, FL.

Finn, J., Ewing, D.J., Ma, L. and Wagner, J. (2010) 'Thermal protection of vehicle payloads using phase change materials and liquid cooling'. *Paper presented at the 2010 American Controls Conference*. *Jun. 30-Jul. 2, 2010*. Baltimore, MD.

Godson, L., Raja, B., Lal, D.M. and Wongwises, S. (2010) 'Enhancement of heat transfer using nanofluids-An overview', *Renewable & Sustainable Energy Reviews*, Vol. 14, No. 2, pp. 629-641.

Huang, H.S., Weng, Y.C., Chang, Y.W., Chen, S.L. and Ke, M.T. (2010) 'Thermoelectric water-cooling device applied to electronic equipment', *International Communications in Heat and Mass Transfer*, Vol. 37, No. 2, pp. 140-146.

Incropera, F.P. and DeWitt, D.P. (1990) *Introduction to Heat Transfer*, New York: John Wiley & Sons.

Kakac, S. and Pramuanjaroenkij, A. (2009) 'Review of convective heat transfer enhancement with nanofluids', *International Journal of Heat and Mass Transfer*, Vol. 52, No. 13-14, pp. 3187-3196.

Leong, K.Y., Saidur, R., Kazi, S.N. and Mamun, A.H. (2010) 'Performance investigation of an automotive car radiator operated with nanofluid-based coolants (nanofluid as a coolant in a radiator)', *Applied Thermal Engineering*, Vol. 30, No. 17-18, pp. 2685-2692.

Lertsatitthanakorn, C., Hirunlabh, J., Khedari, J. and Scherrer, J. (2001) 'Cooling performance of free convected thermoelectric air conditioner'. *Paper presented at the 20th International Conference on Thermoelectrics*. *June 8, 2001*. Beijing, China.

Mitchell, T., Salah, M., Wagner, J. and Dawson, D. (2009) 'Automotive thermostat valve configurations: enhanced warm-up performance', *Journal of Dynamic Systems*

Measurement and Control-Transactions of the ASME, Vol. 131, No. 4, pp. 044501-1-044501-7.

Nguyen, C.T., Desgranges, F., Galanisc, N., Roy, G., Mare, T., Boucher, S. and Mintsa, H.A. (2008) 'Viscosity data for Al2O3-water nanofluid-hysteresis: is heat transfer enhancement using nanofluids reliable?' *International Journal of Thermal Sciences*, Vol. 47, No. 2, pp. 103-111.

Nguyen, C.T., Roy, G., Gauthier, C. and Galanis, N. (2007) 'Heat transfer enhancement using Al2O3-water nanofluid for an electronic liquid cooling system', *Applied Thermal Engineering*, Vol. 27, No. 8-9, pp. 1501-1506.

Pfahnl, A. and Liang, H. (2004) 'Liquid cooling high power compact electronics'. *Paper presented at the Ninth Intersociety Conference on Thermal and Thermomechanical Phenomena in Electronic Systems*. *June 1-4, 2004*. Las Vegas, NV.

Prasher, R., Bhattacharya, P. and Phelan, P.E. (2005) 'Thermal conductivity of nanoscale colloidal solutions (nanofluids)', *Physical Review Letters*, Vol. 94, No. 2, pp. 025901-1-025901-4.

Riffat, S.B. and Ma, X.L. (2003) 'Thermoelectrics: a review of present and potential applications', *Applied Thermal Engineering*, Vol. 23, No. 8, pp. 913-935.

Robinson, A.J. (2009) 'A thermal-hydraulic comparison of liquid microchannel and impinging liquid jet array heat sinks for high-power electronics cooling', *IEEE Transactions on Components and Packaging Technologies*, Vol. 32, No. 2, pp. 347-357.

Simons, R.E. and Chu, R.C. (2000) 'Application of thermoelectric cooling to electronic equipment: A review and analysis'. *Paper presented at the Sixteenth Annual IEEE*

Semiconductor Thermal Measurement and Management Symposium. *Mar. 21-23, 2000*. San Jose, CA.

Simons, R.E., Ellsworth, M.J. and Chu, R.C. (2005) 'An assessment of module cooling enhancement with thermoelectric coolers', *Journal of Heat Transfer-Transactions of the Asme*, Vol. 127, No. 1, pp. 76-84.

Tan, S., Tok, K., Chai, J. and Pinjala, D. (2007) 'Thermal characterization and liquid cooling system integration for stacked modules'. *Paper presented at the 9th Electronics Packaging Technology Conference*. *Dec. 10-12, 2007*. Singapore.

Wang, J., Zou, K. and Friend, J. (2009) 'Minimum power loss control—thermoelectric technology in power electronics cooling'. *Paper presented at the 2009 Energy Conversion Congress and Exposition*. *Sept. 20-24, 2009*. San Jose, CA.

Wang, X.Q. and Mujumdar, A.S. (2007) 'Heat transfer characteristics of nanofluids: a review', *International Journal of Thermal Sciences*, Vol. 46, No. 1, pp. 1-19.

Wong, K.F.V. and Kurma, T. (2008) 'Transport properties of alumina nanofluids', *Nanotechnology*, Vol. 19, No. 34, pp. 345072-1-345072-8.

Wong, K.V. and Castillo, M.J. (2010) 'Heat transfer mechanisms and clustering in nanofluids', *Advances in Mechanical Engineering*, Vol. 14, No. 2, pp. 629-641.

APPENDIX: NOMENCLATURE LIST

A	area, [m^2], state space variable matrix, fitting parameter
B	state space input matrix
C	heat capacity, [J/K]
c_p	specific heat, [J/kg K]
D	diameter of pipe, [m]
d	nanoparticle diameter, [nm]
h	convective heat transfer coefficient, [W/m^2 K]
i	current, [A]
k	conductive heat transfer coefficient, [W/m K]
k_b	Boltzmann constant, [J/K]
m	fitting parameter
n	number of temperature nodes, number of thermoelectric couples
Nu	Nusselt number
P	power, [W]
Pr	Prandtl number
$\dot{Q}$	heat rate, [W]
R	thermal resistance, [K/W]
R_b	interfacial thermal resistance, [Km^2/W]
Re	Reynolds number
T	temperature, [ºC]
V	velocity, [m/s], voltage, [V]
v	velocity, [m/s]
$\bar{u}$	state input vector
$\bar{x}$	state variable vector
Δt	time step, [s]
α	Seebeck coefficient, [μV/K], fluid interfacial parameter
μ	dynamic viscosity, [Pa s]
ν	kinematic viscosity, [m^2/s]
ϕ	volume fraction of nanoparticles
ρ	density, [kg/m^3]

Subscripts

Al	aluminum
avg	average
C	computer chip, cold side
cold	cold side

cool	coolant
D	diameter of pipe [m]
eff	effective
f	base fluid
H	hot side
high	upper thermostat bound
hot	hot side
i	node
in	inner loop
low	lower thermostat bound
N	nanoparticle
out	outer loop
p	nanoparticle
TEC	thermoelectric module
w	water

Tables

Table 1. Summary of model parameters

Symbol	Value	Units	Symbol	Value	Units
A	40,000	-	Pr	3.56	-
$A_{cool,in}$	0.1	m^2	$\dot{Q}_c$	100	W
$A_{cool,out}$	0.3	m^2	R_b	$0.77x10^{-8}$	Km^2/W
A_{TEC}	0.0016	m^2	R_{TEC}	2.0	Ω
cp_{Al}	963	J/kgK	T_{low}	0.5	°C
cp_w	4187	J/kgK	T_{high}	1.5	°C
d	0.00635	m	V	12	V
d_N	$47x10^{-9}$	m	v	0.1	m/s
k_{Al}	180	W/mK	α	-287	μV/K
k_b	$1.38x10^{-23}$	J/K	μ_w	$0.653x10^{-3}$	Ns/ m^2
k_w	0.58	W/mK	ν_w	$0.653x10^{-6}$	m^2/s
k_{TEC}	1.0	W/m^2K	ρ_{Al}	2700	kg/m^3
m	2.5	-	ρ_w	1000	kg/m^3
n	127	-	ϕ	0.0847	-

Table 2. Summary of final results

Case	Fluid	Max T_c (^{0}C)	Max T_{inner} (^{0}C)	Max T_{outer} (^{0}C)	Max h (W/m^2K)	Max Improvement in h (%)
Base Fluid	Water	57	54.9	68.3	959.5	-
Classic	Nanofluid	56.4	54.6	68.3	1114.1	16.1
Brownian	Nanofluid	56.6	54.7	68.3	1059.2	10.4
Fit	Nanofluid	56.6	54.7	68.3	1045.9	9.0

Figure Captions

Figure 1. Size distribution of proposed nanoparticles as ascertained from Transmission Electron Microscope (TEM) pictures

Figure 2. Schematic of thermoelectric concept for heat transfer between the cold and hot device surfaces

Figure 3. Schematic of the vehicle electronic thermal management system design featuring computer chips, thermoelectric devices, and heat exchangers

Figure 4. Computer heat load for a 24 hour cycle in desert conditions

Figure 5. Algorithm flow chart

Figure 6. Computer chip temperature response, TC, for the 24 hour operating period

Figure 7. Temperature dependence of the convective heat transfer coefficient, h, during the 24 hour operating period

Figure 8. Percent improvement of the convection heat transfer coefficient, h, over the base fluid based upon the maximum values

Figures

Figure 1. Size distribution of proposed nanoparticles as ascertained from Transmission Electron Microscope (TEM) pictures

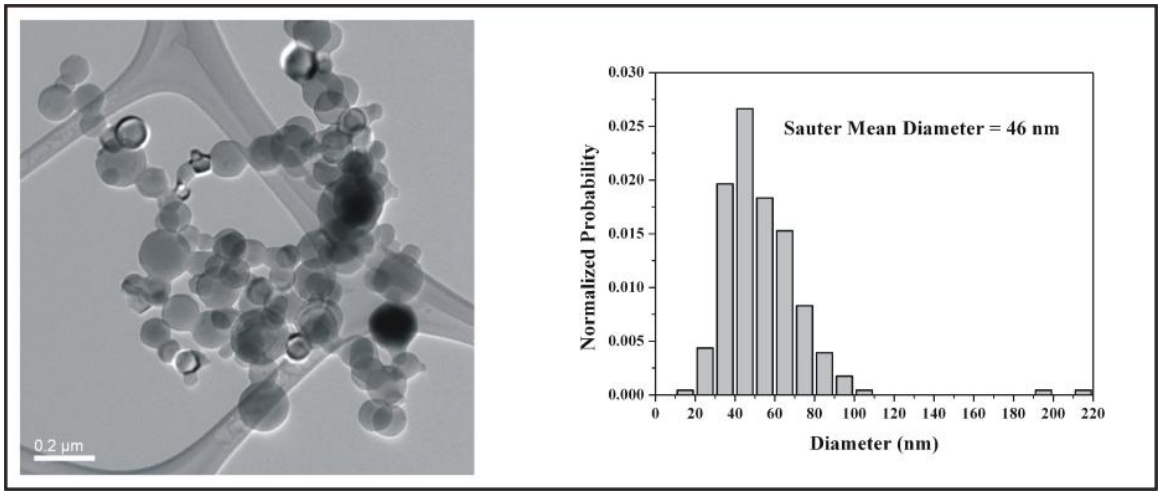

Figure 2. Schematic of thermoelectric concept for heat transfer between the cold and hot device surfaces

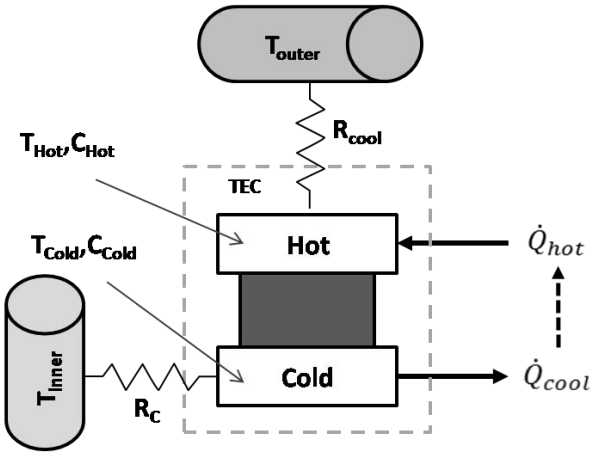

Figure 3. Schematic of the vehicle electronic thermal management system design featuring computer chips, thermoelectric devices, and heat exchangers

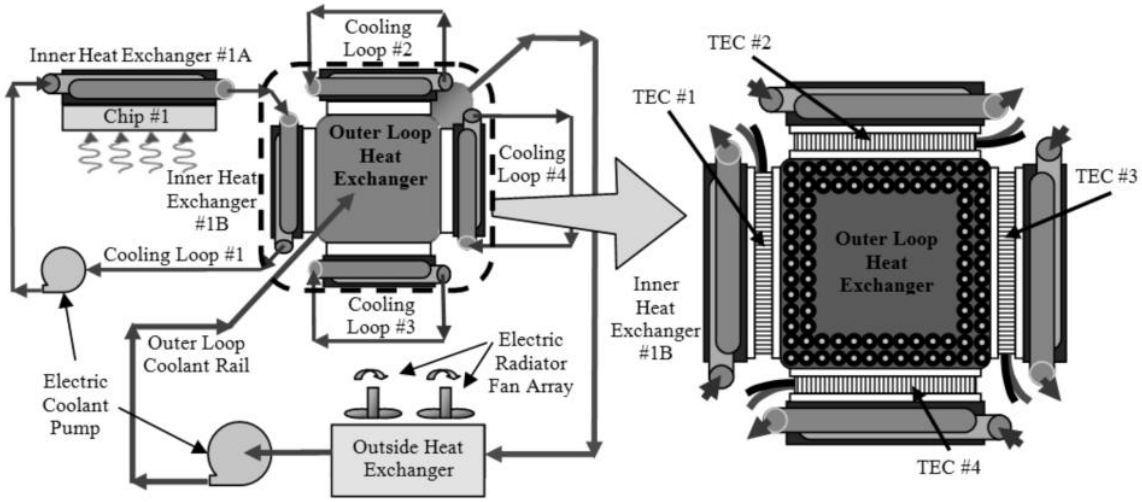

Figure 4. Computer heat load for a 24 hour cycle in desert conditions

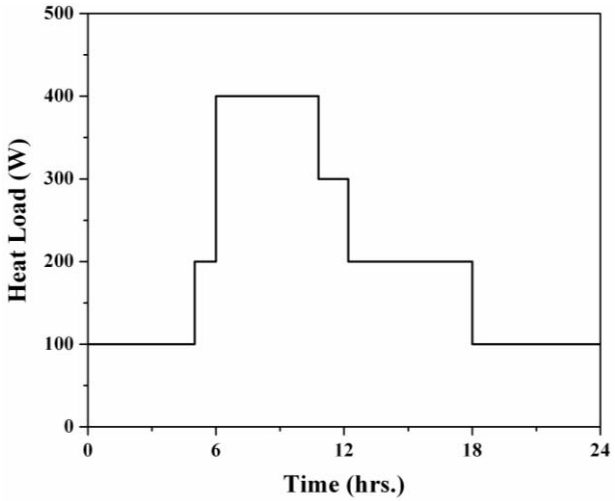

Figure 5. Algorithm flow chart

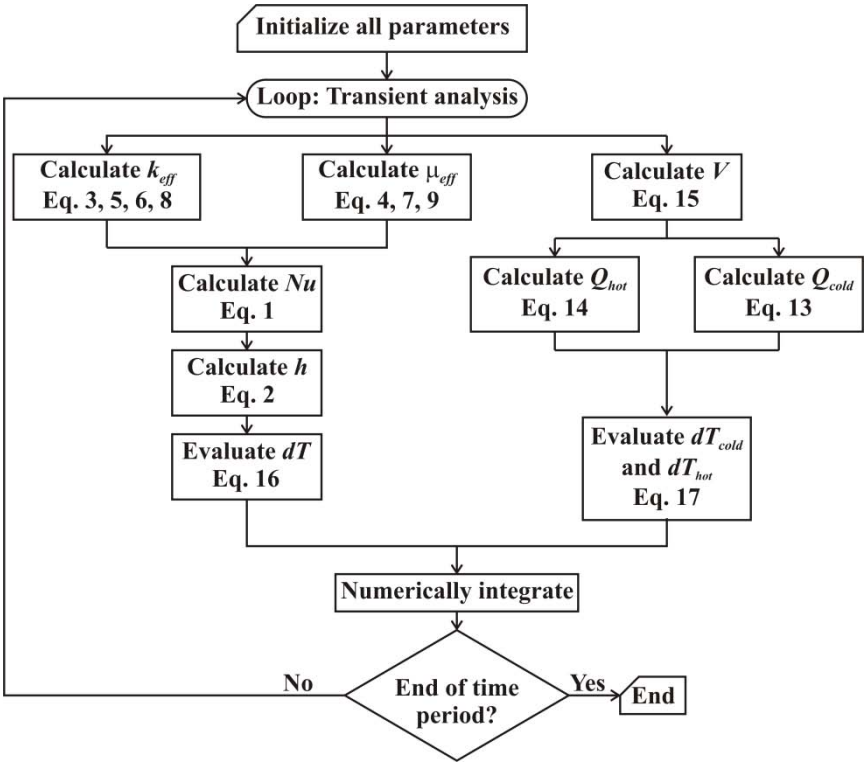

Figure 6. Computer chip temperature response, T_C, for the 24 hour operating period

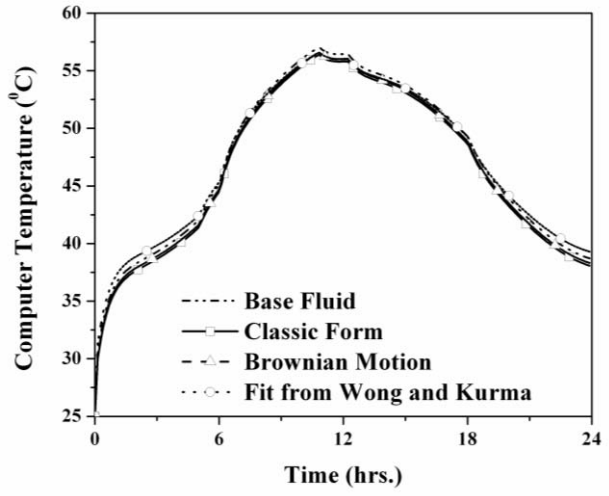

Figure 7. Temperature dependence of the convective heat transfer coefficient, *h*, during the 24 hour operating period

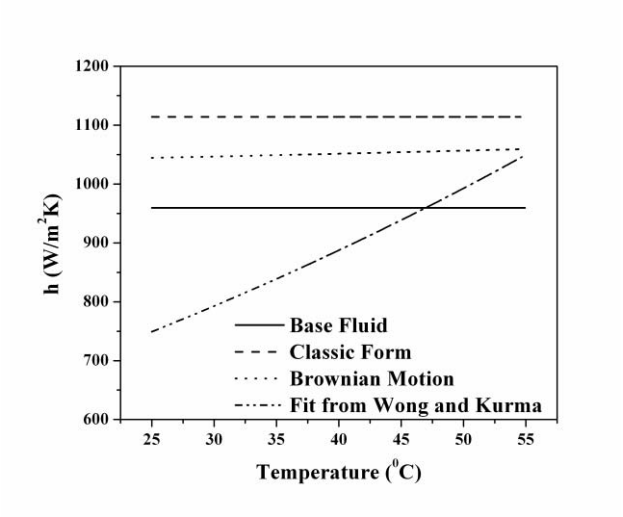

Figure 8. Percent improvement of the convection heat transfer coefficient, *h*, over the base fluid based upon the maximum values